연세대학교 상경대학
경제연구소
Economic Research Institute
Yonsei University

서울시 서대문구 연세로 50
50 Yonsei-ro, Seodaemun-gu, Seoul, Korea
TEL: (+82-2) 2123-4065 FAX: (+82-2) 364-9149
E-mail: yeri4065@yonsei.ac.kr
https://yeri.yonsei.ac.kr

Exact identification, robust inference, and shock masquerading in sign-restricted SVARs

Hyeon-seung Huh
Yonsei University

David Kim
University of Sydney

June 2026
2026RWP-293

Economic Research Institute

Yonsei University

Exact identification, robust inference, and shock masquerading in sign-restricted SVARs

Hyeon-seung Huh
School of Economics
Yonsei University
Republic of Korea
hshuh@yonsei.ac.kr

David Kim
School of Economics
University of Sydney
Australia
Kim.david@sydney.edu.au

Abstract

We propose an alternative sampling scheme for sign-restricted SVARs that addresses two fundamental challenges in the standard approach: prior dependence and shock masquerading. The key idea is to utilize a direct sampling of structural coefficients in the SVAR combined with the robust inference of Giacomini and Kitagawa (2021). The scheme delivers large sets of exactly identified models, and the rotation matrix is uniquely solved via a direct, non-iterative linear algorithm. Sign restrictions are then used as a post-identification filter to ensure economic plausibility. This design is capable of eliminating prior dependence concerns, tightening the credible bounds, mitigating shock masquerading, and improving computational efficiency. We demonstrate the practical utility of the alternative sampling scheme through an application to the U.S. SVAR of Peersman (2005).

Key Words: Structural vector autoregressions, Exact identification, Sign restrictions, Haar prior, Robust inference, Shock masquerading, Givens matrix

JEL Classification: C32, C36, C51, E32, E52

1. Introduction

Structural vector autoregression (SVAR) models identified with sign restrictions allow researchers to encode robust qualitative information (e.g., output must fall in response to a monetary contraction), while avoiding strong parametric assumptions such as short- or long-run zero restrictions. Since sign restrictions take the form of inequality constraints, the procedure does not provide point estimation in the traditional identification scheme, but delivers a set of admissible models, each consistent with both the observed data and the sign restrictions. Despite its popularity, the set-identification approach faces two fundamental and intertwined challenges that may undermine the credibility of its inferences.

The first challenge is prior dependence. Standard implementations typically combine a Normal–Inverse Wishart prior for the reduced-form parameters with a Haar prior for the rotation matrix. Because the Haar prior is never updated by the data, posterior inference may inherit substantial prior influence even asymptotically (Moon and Schorfheide, 2012; Baumeister and Hamilton, 2015, 2018; Giacomini and Kitagawa, 2021). In response, Giacomini and Kitagawa (2021, GK hereafter) propose a robust Bayesian procedure that replaces the unrevisable prior with all possible priors, generating a family of posterior distributions that fully characterize the identified set and its associated uncertainties. The GK procedure eliminates the prior-dependence problem and delivers credible regions that properly account for both sampling uncertainty and identification uncertainty.

The second challenge is the phenomenon of "shock masquerading," elucidated by Wolf (2020, 2022). Under weak sign restrictions, mixtures of non-target shocks may satisfy all the imposed sign restrictions and thus be incorrectly identified as the target shock. This mis-identification could generate impulse responses that may be economically implausible or contradictory. Wolf (2020) finds that shock masquerading can be particularly severe, because the standard Haar-prior procedure tends to give excessive posterior weight to masquerading mixtures. Existing strategies in the literature to curb shock masquerading such as augmenting sign restrictions with external instruments, narrative restrictions, or additional equality/inequality constraints all work by tightening identification and shrinking the set of admissible models to economically plausible regions. To date, empirical extensions have been largely concentrated on specific topics (e.g., monetary and fiscal policy) and may not be readily available for use in other cases.

The aforementioned challenges of prior dependence and shock masquerading arise primarily because sign restrictions are inherently weak identifying devices. By excluding only a limited portion of the admissible structural space, they typically leave a large identified set containing observationally equivalent but economically distinct model representations. This weak identification both heightens sensitivity of posterior inference to the prior over admissible rotations and increases the scope for alternative combinations of shocks to satisfy the same sign pattern, thereby generating shock masquerading. The GK procedure is appealing precisely because the procedure does not conceal this ambiguity through an arbitrary prior choice, as in the standard approach, but instead incorporates it directly into the inferential framework. However, this robustness comes at a cost: when sign restrictions have weak identifying content, the resulting robust credible regions can become very wide and economically uninformative. Consequently, while GK provides a transparent and disciplined characterization of the uncertainty implied by sign restrictions alone, its empirical conclusions may remain too diffuse for precise policy evaluation or sharp structural interpretation. The tension between inferential honesty and empirical sharpness is therefore central to the interpretation of GK results.

This paper proposes an alternative sampling framework that addresses these practical difficulties while preserving a robust treatment of uncertainty in the GK procedure, but at a substantially lower computational cost. The proposed procedure, henceforth the HK scheme, works entirely with exactly identified SVAR representations. Rather than sampling orthogonal rotations, the HK scheme draws contemporaneous coefficients of the SVAR from uniform distributions and treats them as identifying restrictions, solving for all remaining structural parameters, including the rotation matrix, through direct linear algebra. Following the spirit of GK, the scheme computes the minimum and maximum of the accepted responses at each reduced-form draw and then aggregates these endpoints across reduced-form draws to construct credible bands. In a distinct approach, Baumeister and Hamilton (2015) work directly with the contemporaneous coefficients of the SVAR to characterize admissible impulse responses. Their framework assigns explicit priors to these coefficients, some components of which are not updated by the data. As a result, posterior inference may remain sensitive to prior specification. Moreover, by modeling the structural equations directly rather than sampling orthogonal rotations, their approach entails a different parameterization and simulation strategy, including specialized Metropolis-Hastings algorithms, and thus is less naturally embedded into the conventional reduced-form-plus-rotation setup dominant in Bayesian SVAR analysis.[1]

The HK scheme yields several features that distinguish it from the standard sign-restriction framework. First, every accepted model is exactly identified, so the rotation matrix is unique (i.e., singleton) for that model, bypassing the issue of prior dependence in the standard protocol. Because the HK scheme summarizes uncertainty through per-draw minima and maxima, the influence of the uniform draws on structural coefficients is precluded as well. There is an important caveat, however. While the resulting credible bands are robust (in the sense of being independent of the priors over the coefficient support), they typically become tighter than the GK bands. This tightening occurs because the HK procedure explores only the space of exactly identified models, which is a subset of the models generated by sampling over all possible rotations as in the GK scheme. Accordingly, the HK scheme may not capture every single admissible model, but it helps mitigate the overly wide robust band of GK, leading to more economically meaningful inferences in practice.

Second, dealing with exact-identification structure helps alleviate the problem of shock masquerading. Within each exactly identified model, the structural shocks are uniquely pinned down and hence there is no room for shock masquerading in a formal mathematical sense.

[1] Ouliaris and Pagan (2016) develop a non-Bayesian analogue that simulates contemporaneous coefficients in the SVAR to generate candidate impulse responses. Because their algorithm relies on specific distributions for the contemporaneous coefficients that are not updated by the data, the resulting structural inference is inherently sensitive to those distributional choices.

However, the identifying restrictions imposed on the structural coefficients are randomly drawn and do not embody economically meaningful interpretations. Consequently, exact identification alone does not resolve the underlying economic ambiguity in shock interpretation, leaving room for shock masquerading. Put differently, the shock identified from the SVAR model can still be contaminated if the restrictions fail to achieve economic orthogonalization of the underlying structural shocks, thereby producing a biased mixture of true shocks, while the sign restrictions remain insufficiently informative to rule out this mixture. In the empirical section, we construct a "Masquerading Index" that quantifies the degree to which a sign-identified target shock can be mimicked by an admissible mixture of non-target shocks.

Third, the HK scheme offers a substantial computational advantage. Imposing nonzero parametric restrictions on SVAR structural coefficients generally requires iterative nonlinear solvers, since such restrictions define nonlinear constraints. In sign-restricted SVARs, this burden is particularly heavy because the rotation matrix enters the structural coefficients multiplicatively, adding an additional layer of nonlinearity, and the resulting nonlinear system must be solved anew for each of the many thousands of posterior simulation draws. The HK scheme instead delivers a direct, non-iterative algorithm to uniquely identify underlying parameters in the SVAR including those in the rotation matrix. Specifically, the scheme leverages the structure of Givens rotations, which preserves linearity in each SVAR equation with respect to the unknown parameters, allowing for analytical solutions via standard linear algebra. This obviates the use of nonlinear solvers, substantially improving computational efficiency and lowering the practical barriers to conducting robust inference checks. Finally, working in coefficient space enhances economic interpretability: each accepted draw corresponds to a full set of contemporaneous relationships among the variables, enabling a direct inspection of which parameterizations are implausible and which are prone to shock masquerading. This also allows for a rich set of identifying restrictions—inequality/equality restrictions on specific coefficients (e.g., impact elasticities) and other coefficient-level discipline—that can tighten the credible bands and mitigate shock masquerading.

The proposed HK scheme is illustrated in the context of Peersman's (2005) four-variable SVAR for the U.S. economy. His model adopts the standard setup that postulates a normal-inverse Wishart prior for the reduced-form parameters and a Haar prior for the rotation matrix. Section 2 briefly describes the Peersman model and then presents the proposed HK scheme. Section 3 discusses the empirical results of the scheme and makes comparison to those from the standard and GK robust approaches. Section 4 extends the scheme to combine signs with parametric zero restrictions, and the empirical results are reported in Section 5. Section 6 summarizes and concludes the paper.

2. Models

The four-variable SVAR model of Peersman (2005) consists of oil prices (O_t), output (Y_t), and the CPI (P_t) in natural logs, and the short-term interest rate (R_t). He treats the oil price, output, and the CPI as *I*(1) processes and the interest rate as an *I*(0) process. The *I*(1) variables are differenced once so that the vector of variables is $Z_t = \left(\Delta O_t \quad R_t \quad \Delta P_t \quad \Delta Y_t\right)'$. The reduced-form vector moving average representation is expressed as:[2]

$$Z_t = D(L)e_t \tag{1}$$

where $D(L) = (I + D_1 L + D_2 L^2 + \ldots)$, L is the lag operator, and e_t is distributed as $N(0, \Omega)$ so that the reduced-form errors have a mean of zero and are contemporaneously correlated. An initial set of orthogonal shocks is formed as $\varepsilon_t = Pe_t$ where the matrix P^{-1} is such that $\Omega = P^{-1}(P^{-1})'$. In this study, the matrix P^{-1} is obtained from an eigenvalue decomposition of Ω, but it can also be obtained from a Cholesky decomposition of Ω. Equation (1) is written as:

$$Z_t = D(L)P^{-1}Pe_t \tag{2}$$

In Peersman (2005), the Givens matrix is used as the rotation matrix. The initial orthogonal shocks (i.e., Pe_t) are rotated using the Givens matrix, G, which has the property that

[2] The Peersman model includes a constant and time trend, but these deterministic terms are suppressed here for the sake of illustration.

$GG' = G'G = I,$ to form a new set of orthogonal shocks. The orthogonal rotation matrix G is (4x4) as the model has four variables.[3] Now we write equation (2) as:

$$Z_t = D(L)P^{-1}GG'Pe_t \tag{3}$$

The new set of orthogonal shocks is $\eta_t = G'Pe_t,$ and the impulse responses to them are given by:

$$C(L) = D(L)P^{-1}G \tag{4}$$

In the four-variable case (n=4), there are six Givens matrices ($n(n-1)/2$=6). They are $G(\theta_{12}),$ $G(\theta_{13}), G(\theta_{14}), G(\theta_{23}), G(\theta_{24})$, and $G(\theta_{34})$, formed by taking the (4x4) identity matrix and setting $G^{ii}(\theta_{ij}) = \cos\theta_{ij},\ G^{ij}(\theta_{ij}) = -\sin\theta_{ij},\ G^{ji}(\theta_{ij}) = \sin\theta_{ij},\ G^{jj}(\theta_{ij}) = \cos\theta_{ij},$ where the superscripts refer to the row and column of $G(\theta_{ij})$. For example, the Givens matrix $G(\theta_{34})$ is:

$$G(\theta_{34}) = \begin{bmatrix} 1 & 0 & 0 & 0 \\ 0 & 1 & 0 & 0 \\ 0 & 0 & c_{34} & -s_{34} \\ 0 & 0 & s_{34} & \mathrm{c}_{34} \end{bmatrix} \tag{5}$$

where we write c_{ij} short for $\cos\theta_{ij}$ and s_{ij} for $\sin\theta_{ij}$. The Givens matrices are orthogonal, i.e., $G(\theta_{ij})'G(\theta_{ij}) = G(\theta_{ij})G(\theta_{ij})' = I.$ In order to sample as widely as possible from the space of all possible orthogonal matrices, the Givens rotation matrix G in equations (3) and (4) is constructed as the product of the six Givens matrices as:

$$G = [G(\theta_{12})G(\theta_{13})G(\theta_{14})][G(\theta_{23})G(\theta_{24})][G(\theta_{34})] \tag{6}$$

The Givens rotation matrix in equation (6) depends on six different θ_{ij}, and following the convention, Peersman (2005) draws the angles θ_{ij} independently from a uniform density over 0 to π.

[3] Another popular algorithm for forming the rotation matrix is based on Rubio-Ramírez *et al*. (2010), which suggests the QR decomposition of an (nxn) matrix X whose elements are randomly drawn from a *N*(0, 1) distribution. From the QR decomposition of $X = QR$, Q is an orthogonal rotation matrix, and R is an upper triangular matrix.

As in the Peersman (2005), the standard sign-restriction procedure involves drawing reduced-form parameters from the posterior distribution, then generating a large set of candidate structural models by randomly rotating the shocks using an orthogonal rotation matrix. The resulting impulse responses are computed and only those satisfying the sign restrictions are retained, forming the sets of accepted responses from which posterior summaries and credible bands are constructed. By contrast, the GK robust procedure introduces a novel modification to address the fundamental issue of prior dependence. Instead of assuming a single arbitrary prior for the rotation matrix, it searches over the entire class of admissible priors and find the minimum and maximum among the accepted impulse responses at each reduced-form draw. These endpoints are aggregated across reduced-form draws to form rotation-robust credible bands. The trade-off is clear. The standard procedure can deliver tighter, more convenient bands but is rotation-prior dependent and can understate uncertainty, whereas GK's bands are typically much wider and more conservative, with coverage that is immune to the arbitrary influence of any one prior choice at the cost of solving min–max problems.

Unlike the two, the HK scheme begins with sampling contemporaneous coefficients in the SVAR and using them as identifying restrictions to achieve exact identification. Specifically, a set of the contemporaneous coefficients are randomly drawn from uniform distributions, which are often considered "uninformative" or "neutral" in many contexts. The conditions generated by this set of uniform distributions imply a system of equations that can be solved for the unknown angles (i.e., θ_{ij}) in the Givens matrices. The Givens rotation matrix in equation (6) is constructed according to the calculated angles. The number of uniform distributions assumed for the contemporaneous coefficients is three on the first structural equation, two on the second structural equation, one on the third structural equation, and none for the last structural equation. This structure of 3-2-1-0 uniform distributions is consistent with not only the order condition (i.e., $n(n-1)/2$ identifying restrictions) but also the rank conditions for exact identification of the shocks, as derived by Rubio-Ramírez *et al*. (2010). For a given draw, hence, the four shocks underlying the model are exactly identified in the statistical context, and the

Givens rotation matrix is given a unique solution, insusceptible to the prior dependence issue. Economic interpretations to the identified shocks are provided later based on sign restrictions.

When there are four variables in the model, the rotation matrix G in equation (6) has the form:

$$G = \begin{bmatrix} c_{12}c_{13}c_{14} & * & * & * \\ s_{12}c_{13}c_{14} & * & * & * \\ s_{13}c_{14} & * & * & * \\ s_{14} & * & * & * \end{bmatrix} \quad (7)$$

which shows that the first column of G depends only on the angles θ_{12}, θ_{13}, and θ_{14}. Also consider the matrix $\bar{G}$ defined as:

$$\bar{G} = [G(\theta_{23})G(\theta_{24})][G(\theta_{34})] \quad (8)$$

It has the form:

$$\bar{G} = \begin{bmatrix} 1 & 0 & 0 & 0 \\ 0 & c_{23}c_{24} & * & * \\ 0 & s_{23}c_{24} & * & * \\ 0 & s_{24} & * & * \end{bmatrix} \quad (9)$$

The first column is the unit basis vector, and the second column depends only on the angles θ_{23} and θ_{24}. From equations (5), (6), (7), (8), and (9), Fisher and Huh (2020) derive the following results, which we will also use throughout the paper:

Result 1: The first column of the matrix G is identical to the first column of the matrix G_1 where $G_1 = G(\theta_{12})G(\theta_{13})G(\theta_{14})$ and $G = G_1\bar{G}$.[4]

Result 2: The first two columns of the matrix $\bar{G}$ are identical to the first two columns of the matrix G_2 where $G_2 = G(\theta_{23})G(\theta_{24})$ and $\bar{G} = G_2 G(\theta_{34})$.[5]

---

[4] Since $G = G_1\bar{G}$ and the first column of $\bar{G}$ is the unit vector $(1 \quad 0 \quad 0 \quad 0)'$, the first column of G_1 becomes the first column of G.

[5] Since $\bar{G} = G_2 G(\theta_{34})$ and the first two columns of $G(\theta_{34})$ are respectively $(1 \quad 0 \quad 0 \quad 0)'$ and $(0 \quad 1 \quad 0 \quad 0)'$ as in equation (5), the first and second columns of G_2 become the first and second columns of $\bar{G}$.

To formalize the HK scheme, consider the SVAR model corresponding to the vector moving average representation in equations (3) and (4) as:

$$A(L)Z_t = G'Pe_t \tag{10}$$

where $A(L) = C(L)^{-1} = G'PD(L)^{-1} \;\; (\because\; G^{-1} = G')$. Setting $L = 0$ yields the matrix of contemporaneous coefficients as:

$$A(0) = C(0)^{-1} = G'P \quad (\because\; D(0) = I) \tag{11}$$

which measures contemporaneous interactions among the variables. As each of the structural equations is separated by a row, the first structural equation corresponds to the first row of $A(0)$. To identify a structural shock associated with the first equation, the first row of $A(0)$ is normalized on the first variable, and its elements (1,2), (1,3), and (1,4) are randomly drawn from three independent uniform distributions. Collecting all, the first row of $A(0)$ has the form of $U_1 = [1,\, u_{12},\, u_{13},\, u_{14}]$, where u_{12}, u_{13}, and u_{14} are the values drawn from uniform distributions. Obviously, maximum and minimum boundaries are required for each uniform distribution. For these, we use the maximum and minimum values of elements (1,1), (1,2), (1,3), and (1,4) in $G'P$ of equation (11) after simulating G' many times for each reduced-form draw.[6] From $G'P$, each of the elements (1,2), (1,3), and (1,4) is divided by element (1,1), and their individual maximum and minimum values are adopted as the maximum and minimum boundaries of u_{12}, u_{13}, and u_{14}, respectively.

Now, let the first row of G' be a (1x4) vector $\beta_1 = [\beta_{11},\, \beta_{12},\, \beta_{13},\, \beta_{14}]$, and then equation (11) yields $\beta_1 = U_1 P^{-1}$. Using equation (7), the angles θ_{12}, θ_{13}, and θ_{14} determining the first row of G' can be calculated from:

$$\begin{bmatrix}\beta_{11} & \beta_{12} & \beta_{13} & \beta_{14}\end{bmatrix} = \bar{\beta}_1 \begin{bmatrix}c_{12}c_{13}c_{14} & s_{12}c_{13}c_{14} & s_{13}c_{14} & s_{14}\end{bmatrix} \tag{12}$$

[6] We use these simulations purely as a numerical device to approximate the geometric maximum and minimum values of $G'P$. In the limit, those extreme values are determined by P and the geometry of orthogonality with no dependency on the sampling distribution of G (GK, 2021; Ouliaris and Pagan, 2022).

where $\bar{\beta}_1 = \sqrt{\beta_{11}^2 + \beta_{12}^2 + \beta_{13}^2 + \beta_{14}^2}$ is the Euclidean length of β_1. As the vector $[c_{12}c_{13}c_{14} \;\; s_{12}c_{13}c_{14} \;\; s_{13}c_{14} \;\; s_{14}]$ on the right-hand side has a length of one by construction, it is multiplied by $\bar{\beta}_1$ to have the same length as β_1 on the left-hand side. The term $\bar{\beta}_1$ arises because the first row of $A(0)$ is normalized on the first variable, and we return to this later when the full system of equations is established. To extract the angles, divide $\beta_{12} = \bar{\beta}_1 s_{12}c_{13}c_{14}$ by $\beta_{11} = \bar{\beta}_1 c_{12}c_{13}c_{14}$ and use $\tan(\theta_{ij}) = \sin(\theta_{ij}) / \cos(\theta_{ij})$ or in the current notation $t_{ij} = s_{ij} / c_{ij}$ to yield $t_{12} = (\beta_{12} / \beta_{11})$. The solution for θ_{12} becomes:

$$\hat{\theta}_{12} = arc\tan\left(\beta_{12} / \beta_{11}\right) \tag{13}$$

Similarly, divide $\beta_{13} = \bar{\beta}_1 s_{13}c_{14}$ by $\beta_{12} = \bar{\beta}_1 s_{12}c_{13}c_{14}$ and obtain $t_{13} = s_{12}(\beta_{13} / \beta_{12})$ from which the solution for θ_{13} is given as:

$$\hat{\theta}_{13} = arc\tan\left(s_{12}(\hat{\theta}_{12})\beta_{13} / \beta_{12}\right) \tag{14}$$

Finally, divide $\beta_{14} = \bar{\beta}_1 s_{14}$ by $\beta_{13} = \bar{\beta}_1 s_{13}c_{14}$ to obtain $t_{14} = s_{13}(\beta_{14} / \beta_{13})$, and the solution for θ_{14} is given as:

$$\hat{\theta}_{14} = arc\tan\left(s_{13}(\hat{\theta}_{13})\beta_{14} / \beta_{13}\right) \tag{15}$$

Using the calculated angles of $\hat{\theta}_{12}, \; \hat{\theta}_{13},$ and $\hat{\theta}_{14}$, the first row of G' is constructed such that the first row of $A(0)$ is $U_1 = [1, \; u_{12}, \; u_{13}, \; u_{14}]$. This completes the identification of the first shock, and the matrix G_1 in Result 1 is calculated as $G(\hat{\theta}_{12})G(\hat{\theta}_{13})G(\hat{\theta}_{14})$. With the first shock identified, the contemporaneous coefficient matrix of the SVAR model can be rewritten as:

$$A(0) = G'P = \bar{G}'G_1'P \quad (\because \; G = G_1\bar{G}) \tag{16}$$

Using Result 1, the first row of $G'P$ is identical to the first row of $G_1'P$. Further, the first row of $G_1'P$ does not change when pre-multiplied by $\bar{G}'$, the first row of which is a unit vector of $(1 \quad 0 \quad 0 \quad 0)$. Therefore, the first row of $\bar{G}'G_1'P$ contains exactly the same values as the first row of $G'P$ or $A(0)$ for identifying the first shock.

Other structural shocks underlying the model are identified in a similar manner. To identify a shock in the second structural equation, the second row of $A(0)$ is normalized on the second variable, and its elements (2,3) and (2,4) are randomly drawn from two uniform distributions, denoted as u_{23} and u_{24}, respectively. Collect elements (2,2), (2,3), and (2,4) in a vector $U_2 = [1,\ u_{23},\ u_{24}]$. The maximum and minimum boundaries of u_{23} and u_{24} are constructed using the same way as in the case of the first shock.[7] Equation (16) shows that elements in U_2 correspond to the products between the second row of $\bar{G}'$ and the second, third, and fourth columns of $G_1'P$, respectively. From equation (9), let a (1x3) vector $\beta_2 = [\beta_{22}\ \ \beta_{23}\ \ \beta_{24}]$ contain elements in the second row of $\bar{G}'$ except the first one, which is zero. In addition, form a (3x3) submatrix P_2 by deleting row 1 and column 1 of $G_1'P$ (i.e., lower-right 3x3 matrix of $G_1'P$). The vector $\beta_2 = [\beta_{22}\ \ \beta_{23}\ \ \beta_{24}]$ is then calculated as $\beta_2 = U_2 P_2^{-1}$, and the angles determining the second row of $\bar{G}'$ are obtained from:

$$\begin{bmatrix}\beta_{22} & \beta_{23} & \beta_{24}\end{bmatrix} = \bar{\beta}_2 * \begin{bmatrix}c_{23}c_{24} & s_{23}c_{24} & s_{24}\end{bmatrix} \tag{17}$$

where $\bar{\beta}_2 = \sqrt{\beta_{22}^2 + \beta_{23}^2 + \beta_{24}^2}$ is the Euclidean length of β_2. Dividing $\beta_{23} = \bar{\beta}_2 s_{23} c_{24}$ by $\beta_{22} = \bar{\beta}_2 c_{23} c_{24}$ yields $t_{23} = (\beta_{23} / \beta_{22})$, and the solution for θ_{23} is:

$$\hat{\theta}_{23} = arc\tan\left(\beta_{23} / \beta_{22}\right) \tag{18}$$

Likewise, dividing $\beta_{24} = \bar{\beta}_2 s_{24}$ by $\beta_{23} = \bar{\beta}_2 s_{23} c_{24}$ yields $t_{24} = s_{23}(\beta_{24} / \beta_{23})$ from which the solution for θ_{24} is:

$$\hat{\theta}_{24} = arc\tan\left(s_{23}(\hat{\theta}_{23})\beta_{24} / \beta_{23}\right) \tag{19}$$

Using the calculated angles of $\hat{\theta}_{23}$ and $\hat{\theta}_{24}$, the second row of $\bar{G}'$ is constructed such that elements (2,2), (2,3), and (2,4) in the second row of $A(0)$ is $U_2 = [1,\ u_{23},\ u_{24}]$. This completes

[7] From simulating $G'P$ many times for each reduced-form draw, they are the maximum and minimum values of elements (2,3) and (2,4), respectively, after dividing each by element (2,2).

the identification of the second shock, and the matrix $G_2 = G(\hat{\theta}_{23})G(\hat{\theta}_{24})$ in Result 2 is calculated. Then, the contemporaneous coefficient matrix of the SVAR model can be rewritten as:

$$A(0) = \bar{G}'G_1'P = G(\theta_{34})'G_2'G_1'P \qquad (\because \ \bar{G} = G_2G(\theta_{34})) \tag{20}$$

From equation (16), the restrictions for identifying the first shock were contained in the first row of $\bar{G}'G_1'P$. The restrictions for identifying the second shock are contained in the second row of $\bar{G}'G_1'P$. From Result 2, the first two rows of $\bar{G}'G_1'P$ are identical to the first two rows of $G_2'G_1'P$. As the first two rows of $G(\theta_{34})'$ are unit basis vectors, the first two rows of $G(\theta_{34})'G_2'G_1'P$ remain unchanged, sharing the same values in the first two rows of $\bar{G}'G_1'P$ or $A(0)$ for identification of the first two shocks.

To identify the third shock, the third row of $A(0)$ is normalized on the third variable, and its element (3,4) is randomly drawn from a uniform distribution, denoted as u_{34}, making up a (1x2) vector of $U_3 = [1,\ u_{34}]$. In equations (5) and (20), let the last two elements in the third row of $G(\theta_{34})'$ be a (1x2) vector $\beta_3 = [\beta_{33} \quad \beta_{34}]$, and form a (2x2) submatrix P_3 by deleting rows 1 and 2 and columns 1 and 2 of $G_2'G_1'P$. Then, β_3 is calculated as $U_3P_3^{-1}$, and the angle determining the third row of $G(\theta_{34})'$ can be obtained from:

$$\begin{bmatrix}\beta_{33} & \beta_{34}\end{bmatrix} = \bar{\beta}_3 * \begin{bmatrix}c_{34} & s_{34}\end{bmatrix} \tag{21}$$

where $\bar{\beta}_3 = \sqrt{\beta_{33}^2 + \beta_{34}^2}$ is the Euclidean length of β_3. Dividing $\beta_{34} = \bar{\beta}_3 s_{34}$ by $\beta_{33} = \bar{\beta}_3 c_{34}$ gives $t_{34} = (\beta_{34} / \beta_{33})$, and the angle θ_{34} is calculated as:

$$\hat{\theta}_{34} = arc\tan\left(\beta_{34} / \beta_{33}\right) \tag{22}$$

Once $\hat{\theta}_{34}$ is calculated, the rotation matrix G is finally obtained as $G_1G_2G(\hat{\theta}_{34})$ with the four structural shocks fully identified. Taking all the identification restrictions into account, the contemporaneous coefficient of the SVAR model and the impulse response function can be rewritten as:

$$A(0) = \bar{\beta} G' P \tag{23}$$

$$C(L) = D(L) P^{-1} G \bar{\beta}^{-1} \tag{24}$$

where $\bar{\beta}$ is a diagonal matrix of dimension (4x4) with the main diagonal recording the normalization factors $\bar{\beta}_1$, $\bar{\beta}_2$, $\bar{\beta}_3$, and $\bar{\beta}_4$. The first three normalization factors are given in equations (12), (17), and (21), respectively, and the final $\bar{\beta}_4$ is the inverse of element (4,4) in $G'P$. As in the typical simultaneous equation system, the normalization factors serve to render the structural equations such that $A(0)$ or equivalently, $\bar{\beta} G' P$ in equation (23) has a value of one on its main diagonal. The four shocks identified are $\eta_t = \bar{\beta} G' P e_t$ with the size of the shocks being $\bar{\beta}$, and the responses to these shocks can be obtained from equation (24).

The full implementation of the HK scheme is summarized as follows. Step 1 draws reduced-form parameters from their posterior to capture sampling uncertainty, as in the standard and GK procedures. For each reduced-form draw, Step 2 samples the contemporaneous coefficients, u_{12}, u_{13}, u_{14}, u_{23}, u_{24}, and u_{34}, from uniform distributions repeatedly. Step 3 generates a large set of exactly-identified SVAR models by adopting the drawn contemporaneous coefficients as identifying restrictions and solving the Givens rotation matrix G uniquely for the corresponding model based on the algorithm detailed above. One may suspect that the results can be sensitive to the ordering of the variables, just like recursive models (e.g., Cholesky ordering). In the empirical analysis, we take this point into account by randomly selecting the ordering of the variables following the recommendation of Diebold and Yilmaz (2009).[8] Step 4 computes the impulse responses and retain only those draws for which the impulse responses satisfy the sign restrictions. Step 5 computes for each reduced-form draw the minimum and maximum among the accepted impulse responses. Finally, Step 6 is to aggregate these endpoint sequences across reduced-form draws to obtain credible bands. In Steps 5 and 6, the robust

[8] While this random selection is included as a safety measure, our empirical results show that the ordering of the variables does not matter materially.

min-max logic of GK is facilitated to shut down the influence of the uniform draws on the contemporaneous coefficients, thus eliminating prior dependence.

While the scheme is presented in the context of Peersman's model, it can be easily extended to an SVAR of arbitrary dimension owing to the particular structure of the Givens matrices. Taking a five-variable model (n=5) as another example, the rotation matrix G is of the form:

$$\begin{aligned} G &= [G_1][G_2][G_3][G_4] \\ &= [G(\theta_{12})G(\theta_{13})G(\theta_{14})G(\theta_{15})][G(\theta_{23})G(\theta_{24})G(\theta_{25})][G(\theta_{34})G(\theta_{35})][G(\theta_{45})] \end{aligned}$$

and G, $\bar{G} = [G_2][G_3][G_4]$, and $\tilde{G} = [G_3][G_4]$ are respectively given as:

$$G = \begin{bmatrix} c_{12}c_{13}c_{14}c_{15} & * & * & * & * \\ s_{12}c_{13}c_{14}c_{15} & * & * & * & * \\ s_{13}c_{14}c_{15} & * & * & * & * \\ s_{14}c_{15} & * & * & * & * \\ s_{15} & * & * & * & * \end{bmatrix} \quad \bar{G} = \begin{bmatrix} 1 & 0 & 0 & 0 & 0 \\ 0 & c_{23}c_{24}c_{25} & * & * & * \\ 0 & s_{23}c_{24}c_{25} & * & * & * \\ 0 & s_{24}c_{25} & * & * & * \\ 0 & s_{25} & * & * & * \end{bmatrix} \quad \tilde{G} = \begin{bmatrix} 1 & 0 & 0 & 0 & 0 \\ 0 & 1 & 0 & * & * \\ 0 & 0 & c_{34}c_{35} & * & * \\ 0 & 0 & s_{34}c_{35} & * & * \\ 0 & 0 & s_{35} & * & * \end{bmatrix}$$

3. Empirical results with the Peersman sign restriction model

The empirical application follows the specification and dataset of Peersman (2005).[9] The number of accepted responses is set at 500. The sign restrictions utilized by Peersman are reported in Table 1, which distinguish four structural shocks: oil price (OP), aggregate supply (AS), aggregate demand (AD), and monetary policy (MP) shocks. While Peersman does not sign restrict the response of oil prices to an AS shock, he treats the shock with the largest contemporaneous effect on the oil price as the OP shock, which separates the OP shock from the AS shock. The number of quarters over which the sign restrictions are applied to the responses is four for output and CPI (slow-moving variables) and one for the oil price and the interest rate (fast-moving variables).

[9] Peersman uses the quarterly data from 1980:Q1 to 2002:Q2, which can be accessed from the *Journal of Applied Econometrics* data archive at http://qed.econ.queensu.ca/jae/.

Figure 1 reports the main results all together for visual comparison, where the responses are presented in the levels of the series.[10] There are four sets of graphs summarizing the accepted responses to the structural shocks. The first reports the set of posterior means (shaded area), while the second reports the 68% robust credible bounds (red lines), both of which are calculated from the GK procedure. The set of posterior means is computed under all admissible conditional priors consistent with the reduced form and the sign restrictions. It can be viewed as an estimator of the identified set that converges asymptotically to the true identified set (or its convex hull when the true identified set is non-convex). The posterior mean bounds reflect the level of identification uncertainty given the data.[11] The robust credible bounds extend this by incorporating both sampling uncertainty and identification uncertainty across all rotations and priors and hence, can be interpreted as a measure of posterior uncertainty about the identified set.[12] The third reports the 68 percent credible bounds (blue lines) from the standard approach, which are the same as those in the Figure 2 (a) of Peersman (2005). For economic interpretations, we refer the reader to the original paper to conserve space. The last set is the 68 percent credible bounds (black lines) from the HK procedure, which considers only exactly-identified SVAR models but adopts the min-max logic of GK to remove prior dependence over the coefficient support.

The figure shows that the GK robust credible bounds are considerably wider than the credible bounds from the standard approach. The difference represents the combined effect of how the approaches treat structural ambiguity differently. The GK robust credible bounds offer a prior-robust measure of the total uncertainty by encompassing the entire range of structural interpretations that are consistent with the data. In contrast, the standard approach conditions on one particular prior over rotations, so its bands reflect sampling uncertainty but identification uncertainty under that prior only, yielding narrower intervals. Equally important, the credible bounds from the standard approach lie entirely within the GK identified set (i.e.,

[10] In the figure, the graphs are reorganized to have the same ordering as Peersman (2005) for easy comparison.
[11] Sampling noise is largely averaged out by the mean operator in finite samples.
[12] GK show that robust credible region achieves the correct asymptotic coverage for the true identified set if it is convex. Their approach thereby reconciles the asymptotic disagreement between Bayesian and frequentist inference in set-identified models.

the set of posterior means), which can be interpreted as a consistent estimator of the true identified set. This nesting is precisely what the literature warns about in set-identified contexts: the standard approach can remain heavily prior-driven, so credible sets contract to a prior-selected slice of the identified set, producing overly informative inference (Moon and Schorfheide, 2012; Baumeister and Hamilton, 2015, 2018; Giacomini and Kitagawa, 2021). Thus, the standard bands offer convenient sharpness but understate the true scope of uncertainty: it reports a precision that is purely a byproduct of the prior, failing to acknowledge the vast range of alternative structural interpretations that are equally consistent with the data.

The HK scheme produces the credible bounds that are wider than the standard approach by using min–max endpoints à la GK for reflecting the uncertainty. They are tighter than the robust credible bounds from the GK approach. This result is perhaps unsurprising since the HK scheme work only with exactly identified models, which constitutes a subset of the models generated by over all possible rotations considered by GK. Importantly, the HK credible bounds fully contain the GK's identified set across horizons. Possible implications are that the sampling scheme of HK is not susceptible to prior-induced overconfidence in the standard approach, and the tightening relative to the GK robust credible bounds may reflect not the exclusion of admissible models, but rather elimination of economically weak or implausible configurations. Taken together, the results position the HK scheme squarely between two extremes. At one end, the standard method delivers sharp but overly optimistic bands that owe much of their tightness to an arbitrary prior on rotations. At the other end, while the GK procedure attains full robustness by honoring every admissible prior, the resulting bounds can become very wide and less useful for precise policy analysis. The HK scheme trades some of GK's generality for sharper and more informative inference by working only with exactly identified models, yet it remains robust in the sense that it continues to cover the entire GK's identified set. As such, the HK scheme may offer a practically useful alternative for researchers seeking inference that is robust to rotation choices, but with less concern on impractically wide robustness bands and computational costs.

We next turn to the problem of shock masquerading, which can undermine the internal validity of any sign-restriction exercise. As a notable example, Wolf (2020, 2022) demonstrates that under weak sign restrictions, linear combinations of expansionary AD and AS shocks satisfy all sign restrictions and masquerade as contractionary monetary policy shocks. This misidentification generates the familiar output puzzle, in which a monetary tightening appears expansionary. The Peersman (2005) model, which identifies AD, AS, and MP shocks, is hence subject to this scrutiny. To assess vulnerability empirically, we construct a projection-based Masquerading Index (MI) as a proxy of masquerading risk and quantify the extent to which the MP shock is replicable by mixtures of AD and AS shocks. For a given accepted draw, the MI is designed to provide a geometric measure of the proximity between the identified monetary policy shock and the set of admissible mixtures of AD and AS shocks. By construction, it ranges from 0 to 1. A value of 0 means the MP shock is well separated, hence, no evidence of masquerading. A low value indicates that the sign-consistent AD–AS mixture is geometrically distant from the MP response, consistent with a relatively low risk of shock masquerading. A high value means that a mixture of AS and AD shocks can closely replicate the monetary-policy response, indicating more severe shock masquerading. Technical details on this MI are relegated to Appendix to conserve space. Although the impulse responses are generated up to 28 horizons, the MI is computed using the responses only over the horizons used in the sign-restriction scheme: the impact responses of oil prices and the interest rate, and the responses of output and CPI from impact through the subsequent three horizons. This choice deliberately excludes unrestricted longer-horizon responses beyond those for identification because the *MI* aims to evaluate whether mixtures of AD and AS shocks can satisfy the same restrictions that identify the monetary policy shock.

Empirical results for the MI are quite intriguing. Under the standard approach, only 2 of the 500 accepted draws produce nonzero MI values (0.923 and 0.927), which implies that admissible AD–AS mixtures almost never mimic the identified monetary policy shock in the posterior sample (2/500=0.004), even though the two large positive values indicate that masquerading can be sizable when it does occur. The GK results qualify this in an informative way because the lower and upper posterior probabilities of MI>0 are 0 and 0.122, respectively. A lower posterior probability of 0 means that there is always at least one admissible structural interpretation with no masquerading, while an upper posterior probability of 0.122 means that only 12.2% of the accepted draws admit any masquerading at all. The HK approach yields the same qualitative conclusion, but more strongly: while the lower probability remains zero, the upper probability falls to 0.056 (5.6%), meaning that masquerading is admissible for even a smaller fraction of draws. Taken together, the three approaches deliver a consistent message: shock masquerading is not a robust feature, and positive MI is hardly forced by the data. Among them, the GK and HK approaches reveal a small region of structural ambiguity that may be overlooked under the standard approach, while the HK approach suggests weaker empirical exposure to masquerading than the GK approach, likely because it takes only the exactly-identified models.

Wolf (2020) discusses several remedies for shock masquerading. One is the simultaneous identification of multiple shocks, which makes it more difficult for mixtures that mimic the target shock to satisfy the sign restrictions imposed on other shocks. Another is the use of dynamic sign restrictions, which impose sign conditions over multiple horizons, so that impostor shocks that match the target shock on impact fail to match its response path. The Peersman model is amenable to these remedies because all four shocks are identified jointly and the sign restrictions on output and CPI are imposed over several horizons. In particular, the joint identification of shocks appears to be especially helpful in limiting the scope for shock masquerading. To see this intuitively, consider a candidate mixture of AD and AS shocks, $\omega_{AD}C(0)_{AD}+\omega_{AS}C(0)_{AS}$, where ω_{AD} and ω_{AS} are the respective weights, and $C(0)_{AD}$ and $C(0)_{AS}$ denote the vectors of impact responses to the AD and AS shocks across the four variables, respectively. For this mixture to masquerade as the MP shock, its implied sign pattern must agree with the MP restrictions on every variable simultaneously. Inspecting the sign restrictions in Table 1, this is achievable only under $\omega_{AD} \le 0$ and $\omega_{AS} \le 0$. Every other sign configuration fails: if $\omega_{AD} \ge 0$ and $\omega_{AS} \ge 0$, the MP sign restriction on output is violated; If $\omega_{AD} \ge 0$ and $\omega_{AS} \le 0$, or $\omega_{AD} \le 0$ and $\omega_{AS} \ge 0$, then the implied response violates the MP sign restriction on CPI or the interest rate, respectively. Thus, the current setting of sign restrictions narrows the set of admissible AD-AS mixtures that can imitate the MP shock, although the extent of this protection depends on the relative magnitudes of the underlying AD and AS responses. Moreover, because the same sign requirements must also be satisfied by output and CPI at subsequent horizons, the dynamic restrictions may provide an additional safeguard against shock masquerading beyond what can be ruled out using impact restrictions alone.

4. Identification by combining sign and zero restrictions

Given the inherent weakness of sign restrictions, it is useful to examine whether augmenting these qualitative restrictions with stronger parametric zero restrictions on specific responses affects the scope of identification uncertainty. Conceptually, imposing zero restrictions tightens the impulse response identified set by excluding a subset of models that, while satisfying the sign restrictions, violate the mandated zero constraints, thereby potentially yielding more precise inferences. How this reduction in the admissible set is empirically related to the risk of shock masquerading is another interesting venue to explore. Therefore, we extend the HK scheme for sign restrictions detailed in Section 2 to combine with parametric zero restrictions. Previously, Arias *et al*. (2018) and Fisher and Huh (2020) developed a method of imposing zero restrictions in the standard approach that adopts an orthogonal matrix from a QR decomposition or a Givens matrix as the rotation matrix. The prior dependency problem remains, as these rotation matrices can be informative about structural inference. Moreover, because our application imposes multiple nonzero restrictions on the SVAR coefficients, Arias *et al*.'s method is not directly applicable, whereas Fisher and Huh's method would require solving a nonlinear system of equations.

To present the extended HK scheme, the following zero restrictions are in place:

RR1: The MP shock has a zero long-run effect on output.

RR2: The MP shock has a zero contemporaneous effect on output.

RR3: The AD shock has a zero long-run effect on output.

All three restrictions were used in Peersman's (2005) parametric identification case.[13] RR1 and RR3 stem from a vertical long-run aggregate supply curve, while RR2 reflects possible policy lags. To impose these restrictions, recall equation (4) of $C(L) = D(L)P^{-1}G$, from which the long-run response to the structural shocks in η_t is

$$C(1) = D(1)P^{-1}G \tag{25}$$

and the contemporaneous response is

$$C(0) = P^{-1}G \tag{26}$$

There are two zero restrictions on the MP shock (RR1 and RR2). As the first column of G in equation (7) has three free parameters, we treat the first structural shock as the MP shock, and one free parameter is randomly drawn from a uniform distribution to achieve exact identification. Under the current ordering of the variables, RR1 implies that element (4,1) in the long-run response matrix of $C(1)$ is zero, whereas RR2 implies that element (4,1) in the contemporaneous response matrix of $C(0)$ is zero. These are equivalent to assuming that element (1,4) in $G'P^{-T}D(1)'$ for the former and element (1,4) in $G'P^{-T}$ for the latter are zero.

As before, the first row of $A(0)$ corresponding to the first structural equation is normalized on the first variable. Denoting the one free parameter drawn from a uniform distribution by u_{12}, all the restrictions for identifying the MP shock are collected in a (1x4) vector $U_1 = [1 \;\; u_{12} \;\; 0 \;\; 0]$, where the last two zeros present RR1 and RR2. Subsequent steps for implementation are the same as in the case of identification solely by sign restrictions, except for use of an auxiliary matrix M_1 of dimension (4x4). From the relation of $A(0) = C(0)^{-1} = G'P$, fill the first and second columns of M_1 with the first and second columns of P, while the third and fourth columns with the fourth columns of $P^{-T}D(1)'$ and P^{-T}, respectively. Then, letting the first row of G' be a (1x4) vector $\beta_1 = [\beta_{11}, \beta_{12}, \beta_{13}, \beta_{14}]$ yields $U_1 = \beta_1 M_1$, and β_1 is solved as $U_1 M_1^{-1}$. The angles θ_{12}, θ_{13}, and θ_{14} determining the first row of G' can be calculated using equations

[13] The other restrictions he utilized for exact identification were that AS, AD and MP shocks have a zero contemporaneous effect on oil prices.

(12), (13), (14), and (15), just like before. Upon the calculation of $\hat{\theta}_{12},\ \hat{\theta}_{13}$, and $\hat{\theta}_{14}$, the MP shock is identified, and the matrix G_1 in Result 1 is obtained as $G(\hat{\theta}_{12})G(\hat{\theta}_{13})G(\hat{\theta}_{14})$. This identification of the MP shock with the relation of $G = G_1\bar{G}$ can rewrite the long-run and contemporaneous responses of the variables, respectively, as:

$$C(1) = D(1)P^{-1}G = D(1)P^{-1}G_1\bar{G} \tag{27}$$

$$C(0) = P^{-1}G = P^{-1}G_1\bar{G} \tag{28}$$

with the contemporaneous coefficient matrix of the SVAR model as previously shown in equation (16):

$$A(0) = G'P = \bar{G}'G_1'P \tag{16}$$

From equation (27), the long-run restriction RR1 commands element (4,1) in $D(1)P^{-1}G$ to be zero. From Result 1, the first column of $D(1)P^{-1}G$ identifying the MP shock is identical to the first column of $D(1)P^{-1}G_1$. Furthermore, the first column of $D(1)P^{-1}G_1$ does not alter by post-multiplication of $\bar{G}$, the first column of which is a unit vector $(1 \quad 0 \quad 0 \quad 0)'$. Thus, RR1 is maintained in $D(1)P^{-1}G_1\bar{G}$. The same logic applies to the contemporaneous restriction RR2 in equation (28). The zero restriction on element (4,1) in $P^{-1}G$ is carried over to element (4,1) in $P^{-1}G_1\bar{G}$. Finally, in equation (16), the first row of $\bar{G}'G_1'P$ contains exactly the same values as the first row of $G'P$ or $A(0)$ for identification of the MP shock.

Moving to the second structural shock, we treat it as the AD shock which exerts no long-run effect on output by RR3. This leaves one free parameter for exact identification of the AD shock. From equation (27), RR3 sets element (4,2) in $D(1)P^{-1}G_1\bar{G}$ to zero, which is equivalent to assuming that element (2,4) in $\bar{G}'G_1'P^{-T}D(1)'$ is zero. The second row of $A(0)$ corresponding to the second structural equation is normalized on the second variable, and the one free parameter in that equation is randomly drawn from a uniform distribution, denoted by u_{23}. All these restrictions are collected in a (1x3) vector $U_2 = [1 \;\; u_{23} \;\; 0]$, in which the last zero represents RR3. Consider an auxiliary matrix M_2 of dimension (3x3). The first two columns of M_2 are filled with a (3x2) submatrix of $G_1 ' P$ in equation (16) by deleting row 1 and columns 1 and 4. The last column is filled with a (3x1) submatrix of $G_1 ' P^{-T} D(1)'$ by deleting row 1 and columns 1, 2, and 3. Let a (1x3) vector $\beta_2 = [\beta_{22} \;\; \beta_{23} \;\; \beta_{24}]$ contain elements in the second row of $\bar{G}'$, except the first element, which is zero. This yields $U_2 = \beta_2 M_2$, and β_2 is solved as $U_2 M_2^{-1}$. As before, using equations (17), (18), and (19) presents solutions for the angles θ_{23} and θ_{24} determining the second row of $\bar{G}'$. Once $\hat{\theta}_{23}$ and $\hat{\theta}_{24}$ are obtained, the AD shock is identified, and the matrix $G_2 = G(\hat{\theta}_{23}) G(\hat{\theta}_{24})$ in Result 2 is computed.

This identification of the AD shock with the relation of $\bar{G} = G_2 G(\theta_{34})$ can rewrite the long-run and contemporaneous responses, respectively, as:

$$C(1) = D(1) P^{-1} G_1 \bar{G} = D(1) P^{-1} G_1 G_2 G(\theta_{34}) \tag{29}$$

$$C(0) = P^{-1} G_1 \bar{G} = P^{-1} G_1 G_2 G(\theta_{34}) \tag{30}$$

with the contemporaneous coefficient matrix of the SVAR model as previously shown in equation (20):

$$A(0) = \bar{G}' G_1 ' P = G(\theta_{34})' G_2 ' G_1 ' P \tag{20}$$

From the two long-run restrictions RR1 and RR3, elements (4,1) and (4,2) in $D(1) P^{-1} G_1 \bar{G}$ of equation (29) are zero. Elements (4,1) and (4,2) in $D(1) P^{-1} G_1 G_2 G(\theta_{34})$ are also zero because the first two columns of $\bar{G}$ are identical to the first two columns of G_2 by Result 2, and the first two columns of $G(\theta_{34})$ are unit basis vectors. Thus, RR1 and RR3 are maintained in $D(1) P^{-1} G_1 G_2 G(\theta_{34})$. The same mechanism applies for the contemporaneous restriction RR2 in equation (30); hence, the element (4,1) is zero in $P^{-1} G_1 \bar{G}$ and $P^{-1} G_1 G_2 G(\theta_{34})$. Finally, in equation (20), the first two rows of $G(\theta_{34})' G_2 ' G_1 ' P$ contains exactly the same values as the first two rows of $\bar{G}' G_1 ' P$ or $A(0)$ for the identification of MP and AD shocks. Since there is no further zero restriction, the third structural shock can be identified using equations (21) and (22) as before, which provides a solution for the angle θ_{34}. Once $\hat{\theta}_{34}$ is calculated, the identification process is complete and the responses to the structural shocks can be generated from equation (24).[14]

5. Empirical results with sign and zero restrictions

Figure 2 shows the results when the four structural shocks are identified using a combination of sign and three zero restrictions (RR1, RR2, and RR3). For the standard and GK approaches, we adopt the Fisher and Huh (henceforth FH, 2020) procedure that integrates sign and zero restrictions via Givens rotations within the standard single-prior framework. The figure shows that the imposed zero restrictions are clearly visible in the responses. Across all approaches, output responses to the AD and MP shocks converge to zero in the long run as a consequence of RR1 and RR3, while output response to the MP shock is zero on impact, due to RR2. Note that the responses of output to the AD and MP shocks were not sign-restricted, as that was not necessary for identification owing to the two long-run restrictions (RR1 and RR3).[15] Yet, output increases in response to the AD shock at short horizons, which is consistent with standard economic theory. Following the MP shock, a slight output puzzle emerges one quarter after impact.[16]

As expected, all approaches show that strengthening identification through zero restrictions produces substantially tighter bounds relative to sign-only identification, so one can draw more

[14] The HK scheme also accommodates full parametric identification by zero restrictions. Taking the current application as an example, all four structural shocks in the Peersman model can be exactly identified if three zero restrictions are imposed on the first shock, two on the second, and one on the third. This corresponds the number of free parameters in the first column of G, the number in the second column of $\bar{G}$, and the number in the third column of $G(\theta_{34})$. The collection of equations above can be modified accordingly for this full parametric identification, although not shown for conserving space. When the model is exactly identified with zero restrictions, the results are identical to those from the standard procedures for parametric identification models (e.g., Cholesky ordering or IV techniques).

[15] The two long-run restrictions separate the MP and AD shocks from the AS and OP shocks in that the former shocks are restricted to have zero long-run effects on output, whereas the latter are not. The sign restrictions on the responses of oil prices, CPI, and the interest rate in Table 1 separate the MP and AD shocks from each other, thereby no need for restricting the responses of output to the AD and MP shocks by signs.

[16] This also shows up in Peersman's full parametric identification results which utilize two long-run restrictions (RR1 and RR3) and four contemporaneous restrictions, one of which is RR2.

reliable inferences regarding the responses of the variables. The tightening is most pronounced for the AD and MP shocks, as directly pinned down by the zero restrictions. The GK's identified set compresses markedly across responses, consistent with the prediction that zero restrictions substantially narrow down the space of admissible models. Giacomini and Kitagawa (2021) report empirical evidence that the adding zero restrictions substantially tightens the identified set estimates by signs. While the credible bounds from the FH approach also remain narrow, they are mostly tucked inside the GK's identified set, which recalls a lingering issue with prior-dependence and prior-induced overconfidence. In contrast, the HK scheme produces credible bounds that fully encompass the GK's identified set, as visually indicated by shaded regions in the figure, across horizons. Further, the bounds produced by the HK scheme and the GK robust approach are now notably closer to each other. This suggests that when parametric restrictions sufficiently discipline the admissible set, the remaining scope for alternative rotations or sampling schemes becomes limited, yielding convergence toward a common, more conclusive range of accepted responses.

Finally, turning to shock masquerading, the preceding analysis in Section 4 only considered sign restrictions. Now, identification is tightened further by adding a parametric zero restriction: the monetary policy shock is assumed to have no contemporaneous effect on output (RR2). Under this specification, the measured masquerading channel disappears, as the MI is analytically equal to zero. The formal derivation is provided in the Appendix (A-2), but the intuition is straightforward. Once the contemporaneous output-zero restriction is imposed, any admissible AD–AS mixture must also deliver no contemporaneous output response. Because the mixture contains only two shocks, this equality restriction uniquely determines the relative weights of the AD and AS components, leaving a single feasible mixture direction. In our application, neither this direction nor its inverse satisfies the sign pattern required to identify a monetary policy shock. Hence, apart from the trivial zero mixture, no AD–AS combination can masquerade as the monetary policy shock. The admissible set therefore collapses to the zero vector, and the resulting MI is zero. Because this follows directly from RR2, the result holds uniformly across the standard, GK, and HK approaches.

6. Conclusion

We have proposed and demonstrated an alternative sampling scheme for sign-restricted SVARs designed to address the challenges of prior dependence and shock masquerading. The scheme works with exactly identified SVAR models and a direct sampling of contemporaneous structural coefficients, while incorporating the robust min-max logic of Giacomini and Kitagawa (2021) to quantify uncertainty. For implementation, we provide an algorithm that solves all parameters necessary for identification, including the rotation matrix, via direct linear algebra, eliminating the need for iterative nonlinear solvers and the associated computational burden. To tackle shock masquerading, a masquerading index is constructed, which measures how easily a target shock can be replicated by combinations of other shocks.

The empirical application to the Peersman (2005) model reveals several noteworthy findings. First, the credible bands from the standard approach lie entirely within the GK identified set, visually confirming that the apparent precision of the standard inference reflects the influence of a non-updated prior rather than information supplied by the data. Second, our scheme produces bounds that fully cover the GK identified set, indicating robustness to prior specification, while delivering a tighter and more economically informative range of responses than the full robust procedure. Third, the masquerading index suggests that shock masquerading is not a major concern in the Peersman model, owing to its relatively strong identification structure, including multiple identified shocks and dynamic sign restrictions. Compared with the full robust procedure, our scheme indicates the model's empirical exposure to shock masquerading is lower. Finally, these advantages are preserved when sign restrictions are combined with parametric zero restrictions, in which case the scheme continues to provide a balanced and efficient characterization of the admissible set.

Overall, our scheme provides a pragmatic middle ground for practitioners of sign-identified VAR models seeking more precise and economically interpretable policy analyses. While confining to the subspace of exactly identified models, it retains the robustness necessary for credible inference but avoids the excessively wide bounds that can render robust conclusions indecisive. In addition, non-iterative linear algorithm and direct parameter interpretability lower the barrier for conducting sensitivity analysis and for imposing various economic restrictions to sharpen the impulse response identified set and its associated credible bounds.

Appendix

This appendix details how we construct a projection-based masquerading index (MI) that is designed to provide a geometric measure of how closely the identified monetary policy shock is to the set of admissible mixtures of AD and AS shocks. Specifically, it is defined as the norm of the orthogonal projection of the monetary-policy response vector onto that admissible set, normalized by the norm of the monetary-policy response vector itself.

A-1. MI under sign restrictions only

To establish the admissible set for a given accepted draw, each shock response is summarized by a 10-dimensional stacked vector:

$$\lambda_{AD}=\begin{bmatrix} O_{AD,0}\\ R_{AD,0}\\ P_{AD,0}\\ P_{AD,1}\\ P_{AD,2}\\ P_{AD,3}\\ Y_{AD,0}\\ Y_{AD,1}\\ Y_{AD,2}\\ Y_{AD,3}\end{bmatrix},\qquad \lambda_{AS}=\begin{bmatrix} O_{AS,0}\\ R_{AS,0}\\ P_{AS,0}\\ P_{AS,1}\\ P_{AS,2}\\ P_{AS,3}\\ Y_{AS,0}\\ Y_{AS,1}\\ Y_{AS,2}\\ Y_{AS,3}\end{bmatrix},\qquad \lambda_{MP}=\begin{bmatrix} O_{MP,0}\\ R_{MP,0}\\ P_{MP,0}\\ P_{MP,1}\\ P_{MP,2}\\ P_{MP,3}\\ Y_{MP,0}\\ Y_{MP,1}\\ Y_{MP,2}\\ Y_{MP,3}\end{bmatrix}, \tag{A1}$$

where the entries are the responses of oil prices (O), the interest rate (R), CPI (P), and output (Y) to the structural shocks of AD, AS, and MP, where the numbers correspond to the horizons. Using the stacked order above, the desired MP sign pattern is presented in a 10-dimensional stacked vector as:

$$sign=\begin{bmatrix}-1 & +1 & -1 & -1 & -1 & -1 & -1 & -1 & -1 & -1\end{bmatrix}', \tag{A2}$$

and define the diagonal sign-normalization matrix of dimension (10x10) as:

$SIGN$=diag($sign$). (A3)

Then, the sign-normalized monetary policy response is

$$mpr = SIGN\,\lambda_{MP} \geq 0 \tag{A4}$$

because the accepted MP shock already satisfies the restrictions.

Now, collect the responses to AD and AS shocks into a (10x2) matrix:

$$\Xi = [\lambda_{AD} \quad \lambda_{AS}]. \tag{A5}$$

A candidate mixture of AD and AS shocks is

$$\omega_{AD}\lambda_{AD} + \omega_{AS}\lambda_{AS} = \Xi\omega, \tag{A6}$$

where $\omega = (\omega_{AD} \quad \omega_{AS})'$ is the vector of mixture weights. The AD–AS mixture must satisfy the same sign pattern as the monetary policy shock. This means

$$SIGN(\omega_{AD}\lambda_{AD} + \omega_{AS}\lambda_{AS}) = SIGN\,\Xi\omega \geq 0. \tag{A7}$$

Therefore, the admissible set is

$$\Psi = \{\Xi\omega :\ SIGN\,\Xi\omega \geq 0\}. \tag{A8}$$

The MI for a given accepted draw is then defined as

$$MI = \frac{\| \mathrm{P}_{\Psi}(mpr) \|}{\| mpr \|}, \qquad 0 \leq MI \leq 1, \tag{A9}$$

where ||•|| denotes the Euclidean norm, and $\mathrm{P}_{\Psi}(mpr)$ is the orthogonal projection of the monetary-policy response vector mpr in equation (A4) onto the admissible set Ψ in equation (A8). Since Ψ is closed and convex under weak inequalities, this projection is well defined. Equivalently, MI may be obtained by solving a standard convex quadratic programming problem that minimizes the distance between mpr and the admissible mixture $\Xi\omega$ as

$$\hat{\omega} = \arg\min_{\omega} \| mpr - \Xi\omega \|^2 \tag{A10}$$

subject to the corresponding sign restrictions of $SIGN\,\Xi\omega \geq 0$, and then setting

$$MI = \frac{\| \Xi\hat{\omega} \|}{\| mpr \|}. \tag{A11}$$

The MI ranges from 0 to 1. A value of zero means the MP shock (target shock) is well separated, hence, no admissible masquerading. A larger MI means that the identified monetary policy shock lies closer to the region spanned by impostor shock mixtures, indicating more severe shock masquerading.

A-2. *MI* under sign restrictions and one zero restriction

We now add the parametric restriction that the monetary policy shock has no contemporaneous effect on output, $Y_{MP,0} = 0$ in the λ_{MP} vector of (A1). Accordingly, the impact output sign restriction is not imposed. The output sign restrictions apply only at the horizons of one to three. Reflecting this, define the 9-dimensional stacked response vector:

$$\lambda_{AD} = \begin{bmatrix} O_{AD,0} \\ R_{AD,0} \\ P_{AD,0} \\ P_{AD,1} \\ P_{AD,2} \\ P_{AD,3} \\ Y_{AD,1} \\ Y_{AD,2} \\ Y_{AD,3} \end{bmatrix}, \qquad \lambda_{AS} = \begin{bmatrix} O_{AS,0} \\ R_{AS,0} \\ P_{AS,0} \\ P_{AS,1} \\ P_{AS,2} \\ P_{AS,3} \\ Y_{AS,1} \\ Y_{AS,2} \\ Y_{AS,3} \end{bmatrix}, \qquad \lambda_{MP} = \begin{bmatrix} O_{MP,0} \\ R_{MP,0} \\ P_{MP,0} \\ P_{MP,1} \\ P_{MP,2} \\ P_{MP,3} \\ Y_{MP,1} \\ Y_{MP,2} \\ Y_{MP,3} \end{bmatrix}, \qquad \text{(A1)'}$$

where the excluded elements are $Y_{AD,0}$, $Y_{AS,0}$, and $Y_{MP,0}$. The monetary-policy sign vector of dimension (9x1) is

$$sign = \begin{bmatrix} -1 & +1 & -1 & -1 & -1 & -1 & -1 & -1 & -1 \end{bmatrix}'. \qquad \text{(A2)'}$$

Define the diagonal sign-normalization matrix of dimension (9x9) as

SIGN=diag(*sign*). (A3)'

The rests of the procedure are carried out in the same fashion as the case of only sign restrictions, after adjusting the reduced number of parameters, including that $\Xi = [\lambda_{AD} \quad \lambda_{AS}]$ in (A5) is now of dimension (9x2). The exception is the admissible set in (A8). Following the parametric restriction of $Y_{MP,0} = 0$, a masquerading AD–AS mixture should also satisfy the same contemporaneous output-zero restriction:

$$\omega_{AD} Y_{AD,0} + \omega_{AS} Y_{AS,0} = 0. \qquad \text{(A12)}$$

Define

$\xi = [y_{AD,0} \quad y_{AS,0}]$. (A13)

Then the restriction can be written as:

$\xi\omega = 0$.

The admissible set becomes

$\Psi = \{\Xi\omega: \ SIGN\Xi\omega \geq 0, \ \xi\omega = 0\}$. (A8)’

The MI for a given accepted draw is calculated using (A9), or equivalently, (A10) and (A11) subject to the sign and parametric zero restrictions of $SIGN\Xi\omega \geq 0$ and $\xi\omega = 0$. A low value of MI means that the zero-restriction-consistent AD-AS mixture is far from the monetary-policy response, whereas a high value means that the AD-AS mixture can replicate the monetary-policy response while respecting the contemporaneous output-zero restriction.

For the application at hand, however, the mixture weights of ω_{AD} and ω_{AS} can be easily solved analytically. This is because the contemporaneous output-zero restriction in (A12) removes one degree of freedom as:

$\omega_{AS} = -\omega_{AD}[y_{AD,0} / y_{AS,0}]$ (A14)

Substituting (A14) into the sign restrictions for CPI and the interest rate at impact yields

$\omega_{AD}P_{AD,0} + \omega_{AS}P_{AS,0} = \omega_{AD}[P_{AD,0} - P_{AS,0}(Y_{AD,0} / Y_{AS,0})] \leq 0$ (A15)

$\omega_{AD}R_{AD,0} + \omega_{AS}R_{AS,0} = \omega_{AD}[R_{AD,0} - R_{AS,0}(Y_{AD,0} / Y_{AS,0})] \geq 0$ (A16)

For the right-hand expressions in (A15) and (A16), the sign restrictions in imposition are $P_{AD,0} \geq 0$, $P_{AS,0} \leq 0$, $R_{AD,0} \geq 0$, $R_{AS,0} \leq 0$, and $(Y_{AD,0} / Y_{AS,0}) \geq 0$. Thus, both bracketed terms are nonnegative, and generically strictly positive unless one is on a boundary case. Then, (A15) requires $\omega_{AD} \leq 0$, while (A16) requires $\omega_{AD} \geq 0$. The only feasible solution for this case is $\omega_{AD} = 0$, and the same is true for ω_{AS}, i.e., $\omega_{AS} = 0$ by (A14). Thus, the only feasible mixture is the trivial one, implying that the admissible set collapses to the singleton $\Psi = \{0\}$ and $MI = 0$. For the present application, shock masquerading is ruled out by construction in that no nontrivial mixture of AD and AS shocks can satisfy both the zero restriction and the required sign pattern.

References

Arias, J. E., J. F. Rubio-Ramírez, and D. F. Waggoner, 2018, Inference based on structural vector autoregressions identified with sign and zero restrictions: Theory and applications, *Econometrica* 86, 685-720.

Baumeister, C. and J. Hamilton, 2015, Sign restrictions, structural vector autoregressions, and useful prior information, *Econometrica* 83, 1963-1999.

Baumeister, C. and J. Hamilton, 2018, Inference in structural vector autoregressions when the identifying assumptions are not fully believed: Re-evaluating the role of monetary policy in economic fluctuations, *Journal of Monetary Economics* 100, 48-65.

Diebold F. and K. Yilmaz, 2009, Measuring financial asset return and volatility spillovers, wth application to global equity markets, *Economic Journal* 119, 158–171.

Fisher, L. and H-S. Huh, 2020, Combining sign and parametric restrictions in SVARs by utilising Givens rotations, *Studies in Nonlinear Dynamics & Econometrics* 24, 1-19.

Giacomini R. and T. Kitagawa, 2021, Robust Bayesian inference for set-identified models, *Econometrica* 89, 1519-1556.

Moon, H. and F. Schorfheide, 2012, Bayesian and frequentist inference in partially identified models, *Econometrica* 80, 755-782.

Ouliaris S. and A. Pagan, 2016, A method for working with sign restrictions in structural equation modeling, *Oxford Bulletin of Economics and Statistics* 78, 605-622.

Peersman G., 2005, What caused the early millennium slowdown? Evidence based on vector autoregressions, *Journal of Applied Econometrics* 20, 185-207.

Rubio-Ramírez, J. F., D. F. Waggoner, and T. Zha, 2010, Structural vector-autoregressions: Theory of identification and algorithms for inference, *Review of Economic Studies* 77, 665-696.

Wolf, C., 2020, SVAR (Mis)identification and the Real Effects of Monetary Policy Shocks, *American Economic Journal: Macroeconomics* 12, 1–32.

Wolf, C., 2022, What can we learn from sign-restricted VARs?, *AEA Papers and Proceedings,* 112, 471-475.

Table 1: Sign restrictions

Shock\Variable	Oil Price	Output	CPI	Interest rate
Oil price shock	≥0	≤0	≥0	≥0
Aggregate supply shock	?	≥0	≤0	≤0
Aggregate demand shock	≥0	≥0	≥0	≥0
Monetary policy shock	≤0	≤0	≤0	≥0

Note: The designation '?' denotes an unrestricted response.

Figure 1: Full sign restriction identification

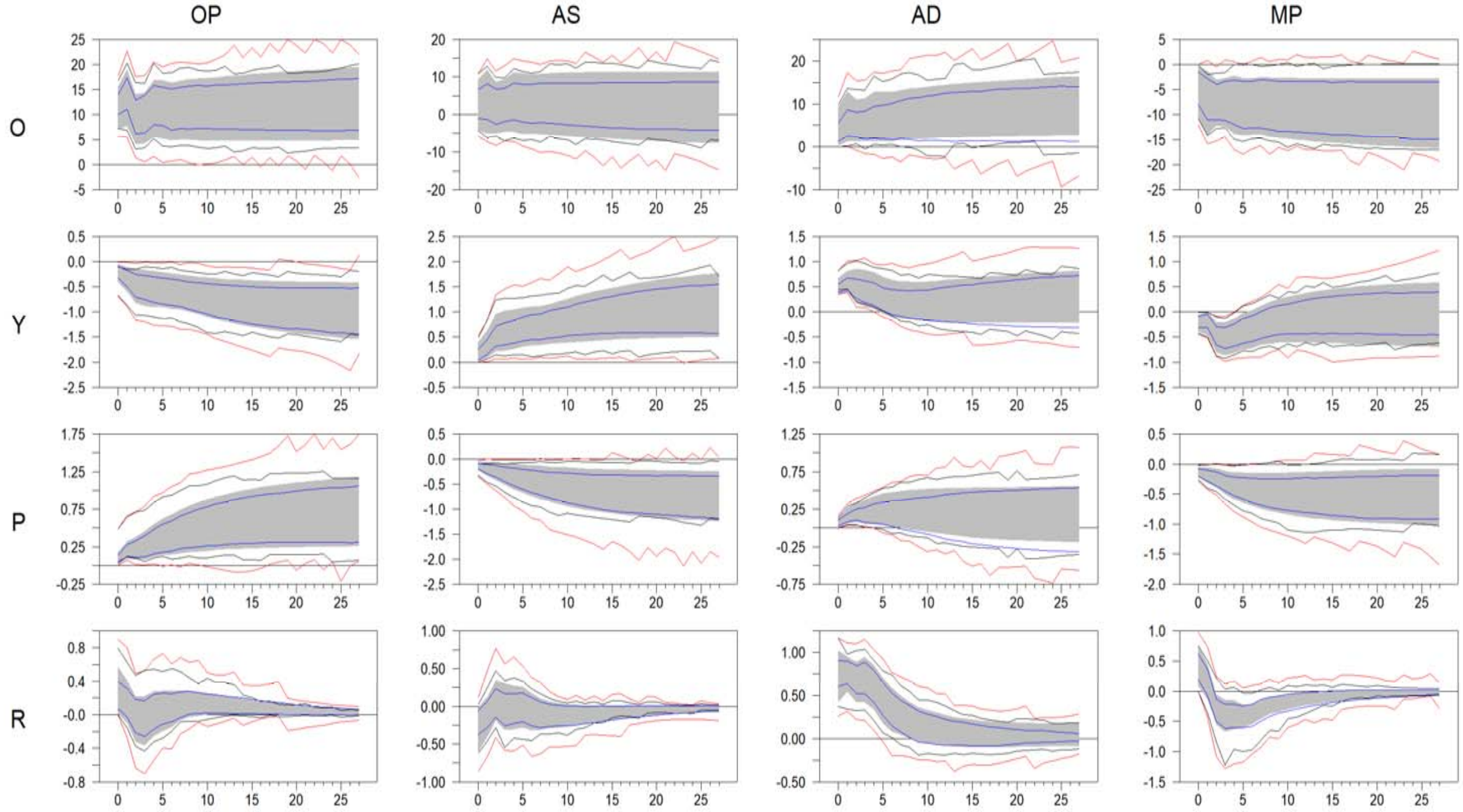

Notes: Shaded regions depict the set of posterior means generated using the GK procedure. Blue, black, and red lines depicts the 68% credible bands from the standard, HK, and GK procedures, respectively.

Figure 2: Sign and zero restriction identification

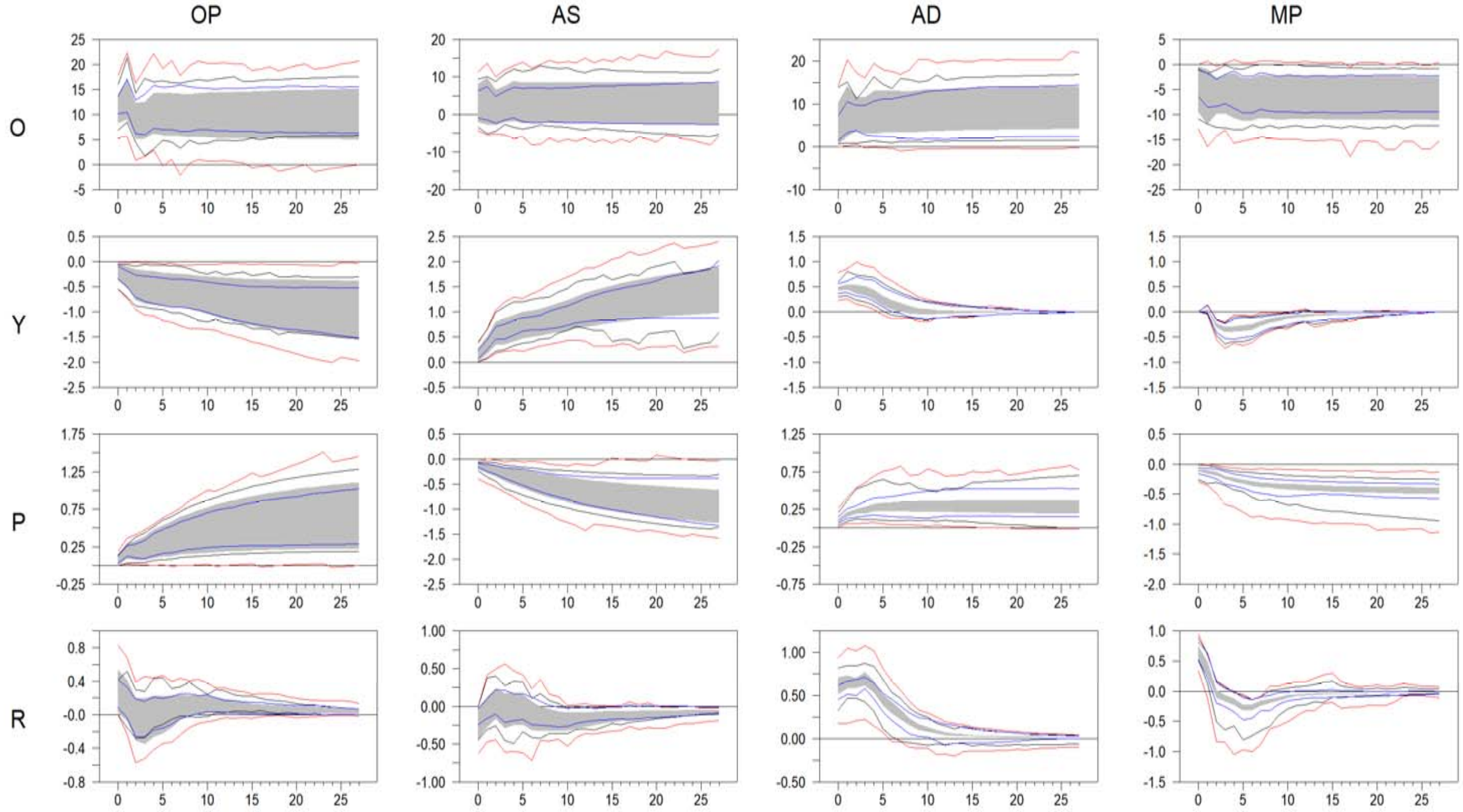

Notes: Shaded regions depict the set of posterior means generated using the GK procedure. Blue, black, and red lines depict the 68% credible bands from the FH, HK, and GK procedures, respectively.